

## Supplementary information

### The low-temperature synthesis of cation-ordered Ce-Zr-based oxide via an intermediate phase between Ce and Fe

Kazuto Murakami,<sup>a</sup> Yoko Sugawara,<sup>a</sup> Junki Tomita,<sup>a</sup> Akihiro Ishii,<sup>a</sup> Itaru Oikawa,<sup>a</sup> and Hitoshi Takamura\*<sup>a</sup>

<sup>a</sup> Department of Materials Science, Graduate School of Engineering, Tohoku University, Sendai 980-8579, Japan.

\* Corresponding author email: takamura@material.tohoku.ac.jp

**Table S1** Chemical composition of CZ55, CZ55-xCFOs, and CZ55-5vol%Fe<sub>2</sub>O<sub>3</sub> or Co<sub>3</sub>O<sub>4</sub>.

Nominal composition	Ce (mol%)	Zr (mol%)	Co (mol%)	Fe (mol%)	Ce/Zr	Fe/Co
Ce <sub>0.5</sub> Zr <sub>0.5</sub> O <sub>2</sub> (CZ55)	50.8	49.2	0.00	0.03	1.03	-
CZ55-1CoFe <sub>2</sub> O <sub>4</sub> (1CFO)	48.6	49.3	0.74	1.38	0.99	1.87
CZ55-2CoFe <sub>2</sub> O <sub>4</sub> (2CFO)	48.1	48.6	0.93	2.38	0.99	2.55
CZ55-3CoFe <sub>2</sub> O <sub>4</sub> (3CFO)	47.1	47.5	1.82	3.54	0.99	1.95
CZ55-4CoFe <sub>2</sub> O <sub>4</sub> (4CFO)	45.3	47.7	2.14	4.83	0.95	2.26
CZ55-5CoFe <sub>2</sub> O <sub>4</sub> (5CFO)*	47.6	44.7	2.12	5.52	1.06	2.61
CZ55-5vol%Co <sub>3</sub> O <sub>4</sub>	45.7	46.3	7.77	0.23	0.99	-
CZ55-5vol%Fe <sub>2</sub> O <sub>3</sub>	46.0	47.2	0.00	6.89	0.97	-

\*Nominal cation composition of 5CFO, i.e. (CeZrO<sub>4</sub>)<sub>95</sub>-(CoFe<sub>2</sub>O<sub>4</sub>)<sub>5</sub>, is Ce<sub>46.34</sub>Zr<sub>46.34</sub>Co<sub>2.44</sub>Co<sub>4.88</sub>.

**Table S2** Specific surface area of CZ, CZ-xCFOs, and CZ-5vol%Fe<sub>2</sub>O<sub>3</sub> after reduction.

Sample	SSA / m <sup>2</sup> /g	Size / nm	Note
Ce <sub>0.5</sub> Zr <sub>0.5</sub> O <sub>2</sub> (CZ55)	22.3	40.6	Pechini
CZ55-1CoFe <sub>2</sub> O <sub>4</sub> (1CFO)	14.4	63.2	Pechini
CZ55-5CoFe <sub>2</sub> O <sub>4</sub> (5CFO)	12.7	71.4	Pechini
CZ55-5vol%Fe <sub>2</sub> O <sub>3</sub>	5.2	175	κ-phase, after reduction@800°C, 1h
CZ55-5vol%Fe <sub>2</sub> O <sub>3</sub>	3.8	324	κ-phase, after reduction@800°C, 5h
CZ55	2.7	336	κ-phase, after reduction@1200°C, 5h

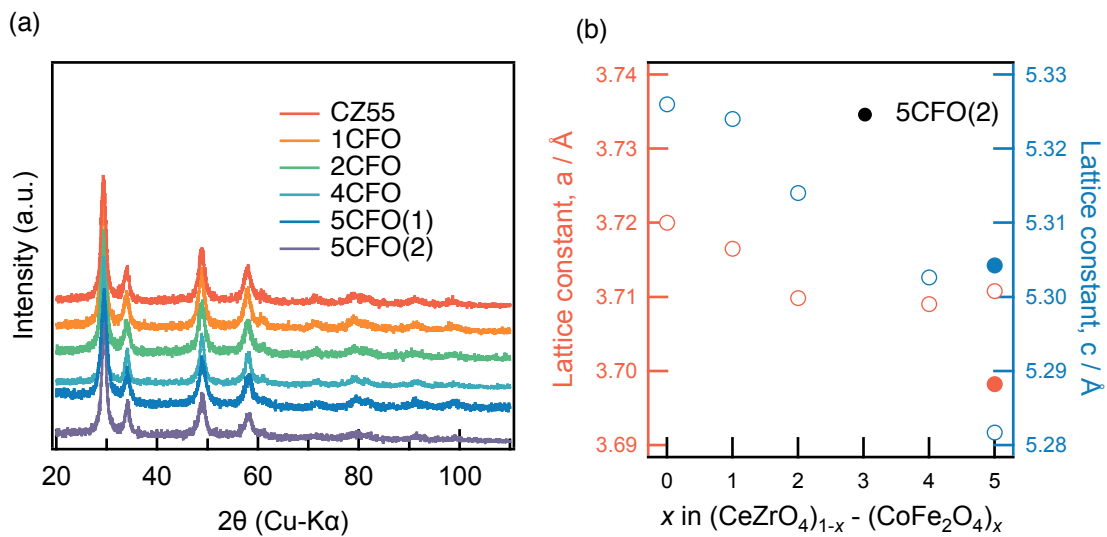


**Fig. S1** (a) XRD patterns and (b) lattice constant of 1-5CFO powders after calcination at 800 °C for 2 h.

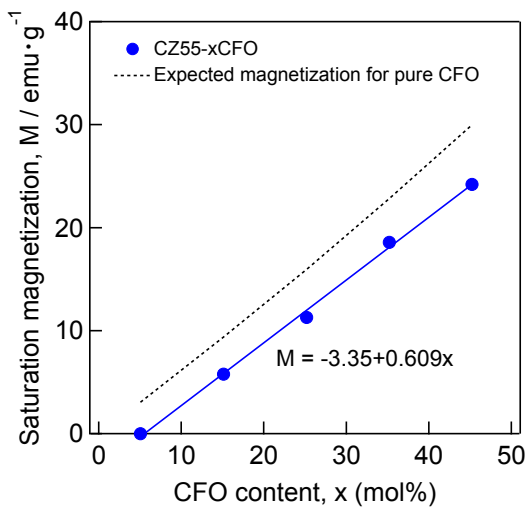


**Fig. S2** Magnetization as a function of CFO content.

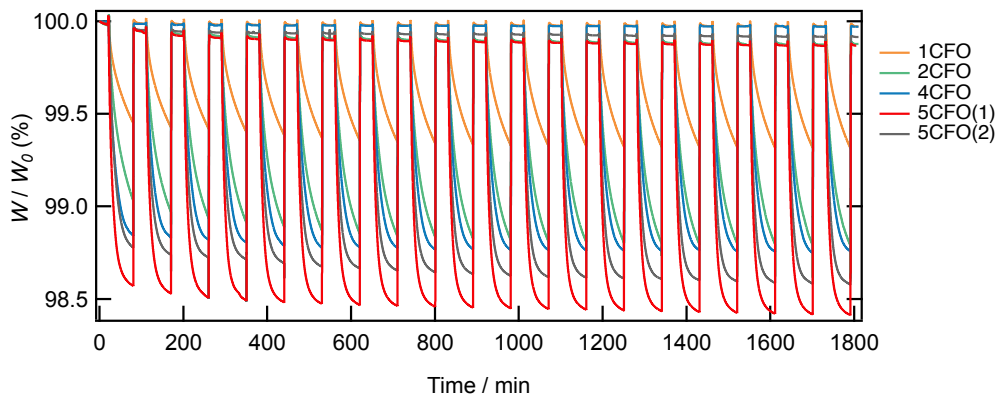


**Fig. S3** TGA curves in a long-term cyclic experiment of 1-5CFO at 400 °C.

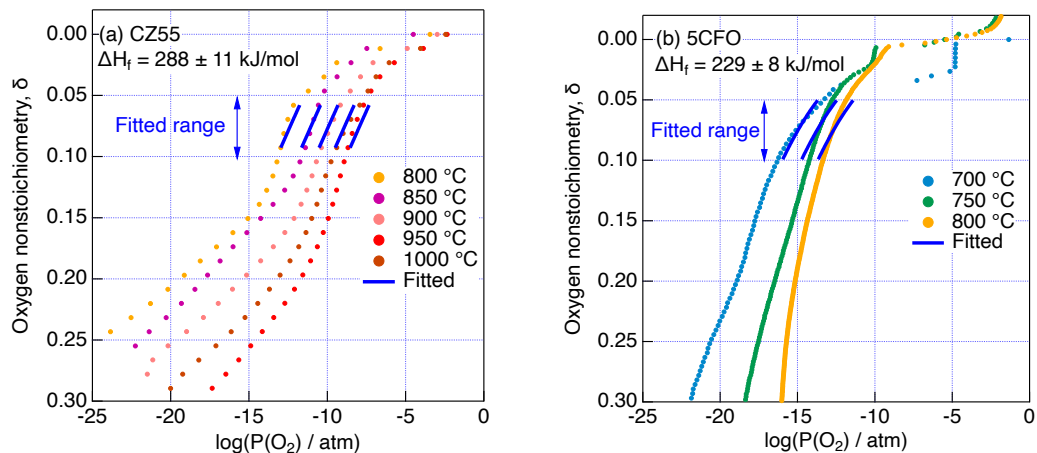


**Fig. S4** Temperature dependence of oxygen nonstoichiometry,  $\delta$  of (a) CZ55 and (b) 5CFO(1) as a function of oxygen partial pressure. A range of  $\delta$  for fitting is between 0.05 and 0.1 as shown by blue arrows.

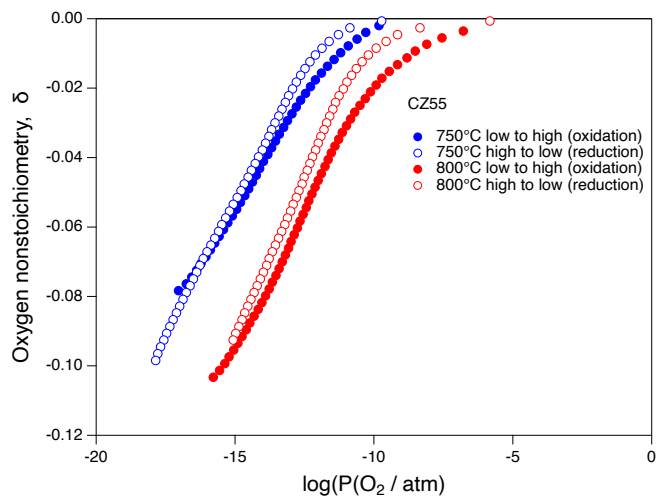


**Fig. S5** Reversible titration tests for CZ55 at 750 and 800 °C. Even though the oxidation and reduction curves do not perfectly match, hysteresis is not so significant. In principle, a

smaller titration current and more rigorous convergence criteria should give more reversible curves (smaller hysteresis). Meanwhile, inevitable gas (mechanical and electrochemical) leakages, which are fatal for a very small dead-volume cell with no buffer-effect gas, need to be minimized by shortening the measurement time. Under this circumstance, titration conditions were optimized, as described in the experimental section.

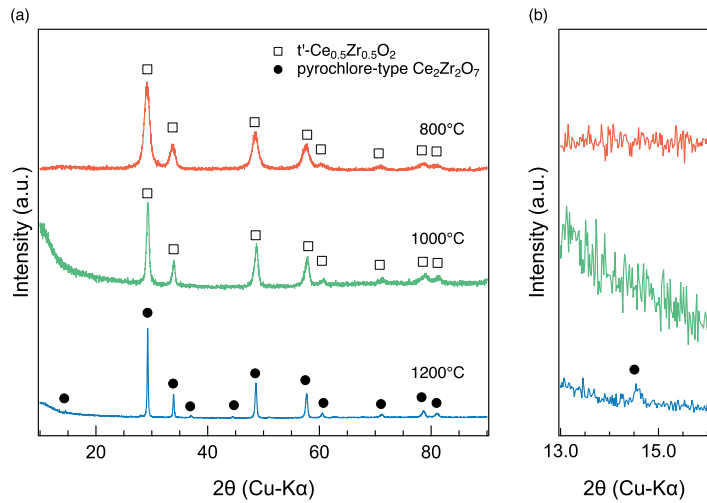


**Fig. S6** XRD patterns of CZ55 reduced in Ar-5%H<sub>2</sub> at 800, 1000, and 1200 °C. The cation-ordered phase (pyrochlore-type) cannot be obtained below 1200 °C without doping.

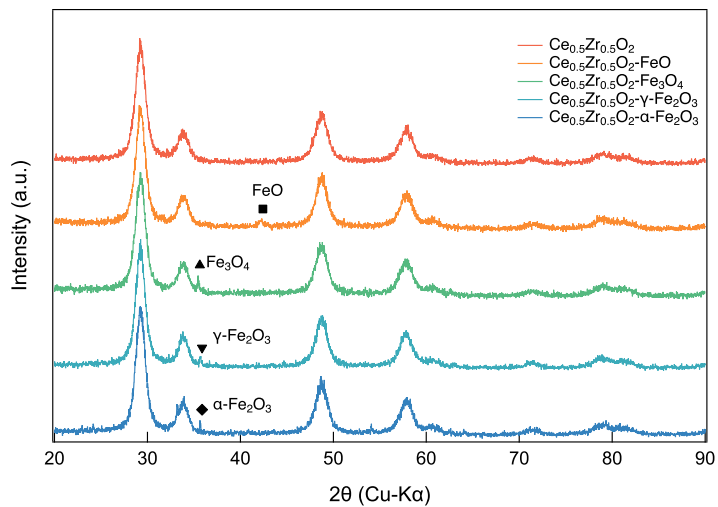


**Fig. S7** XRD patterns of  $\text{Ce}_{0.5}\text{Zr}_{0.5}\text{O}_2$  (CZ55) and iron-oxide-added CZ55. 5-vol%iron oxides were mechanically mixed with CZ55. In addition to  $\alpha\text{-Fe}_2\text{O}_3$ ,  $\gamma\text{-Fe}_2\text{O}_3$ ,  $\text{Fe}_3\text{O}_4$ , and FeO were examined.

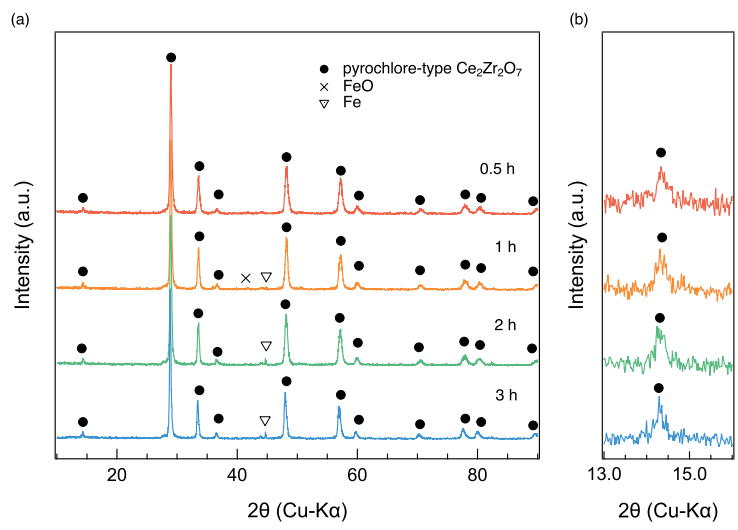


**Fig. S8** (a) XRD patterns of CZ55 with 5 vol% $\gamma$ - $\text{Fe}_2\text{O}_3$  after reduction at 800 °C for 0.5 to 3 h under Ar-5%H<sub>2</sub>. An ordered peak area around 14° is shown in (b).

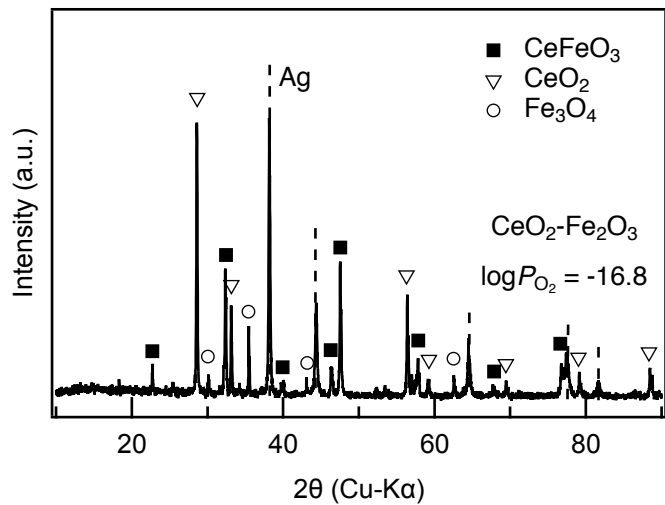


**Fig. S9** XRD pattern of Ce-Fe mixed oxide after coulometric titration at 800 °C.

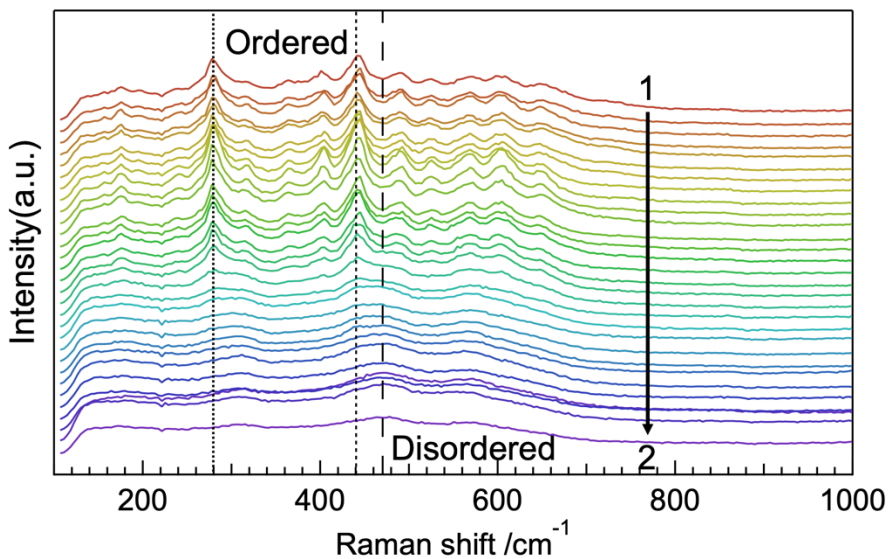


**Fig. S10** Raman spectra taken for CZ55 powders coated with  $\text{Fe}_2\text{O}_3$  after reduction at 900 °C for 5 h. The spectra were taken from area 1 (top) to 2 (bottom) shown in Fig. 9(a). Strong peaks at 280 and 440  $\text{cm}^{-1}$  are attributed to the ordered phase.

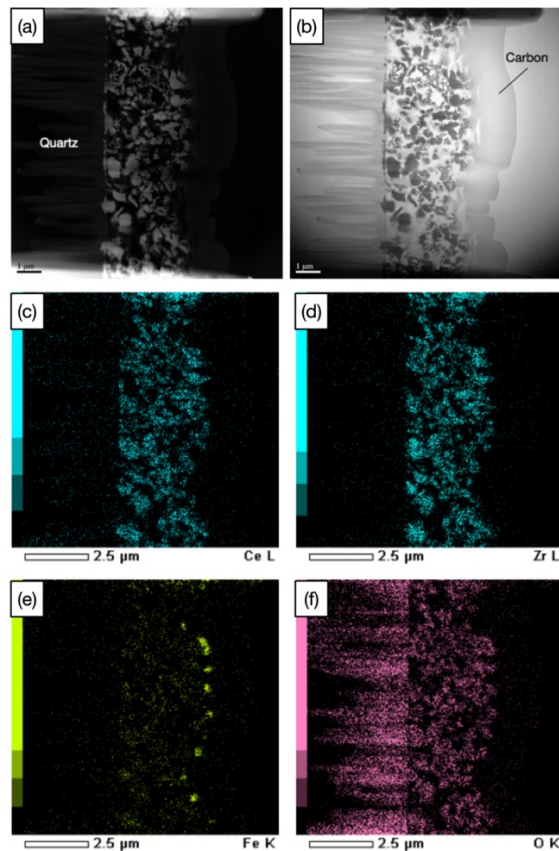


**Fig. S11** Cross-sectional (a) STEM-ADF and (b) ABF images of  $\alpha\text{-Fe}_2\text{O}_3$ -coated CZ55 powders, and its elemental mapping of (c) Ce, (d) Zr, (e) Fe, and (f) O.

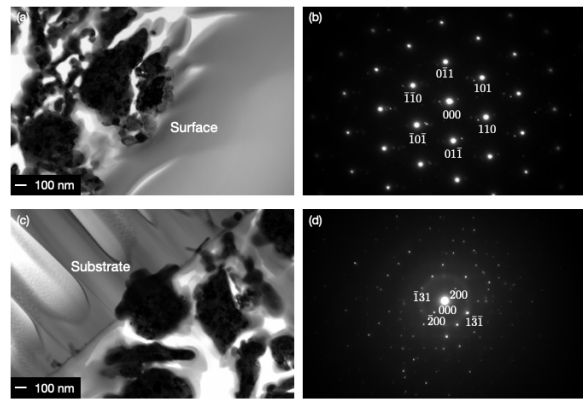


**Fig. S12** STEM-ADF images of (a) near the surface and (c) substrate. (b) and (d) are electron diffraction (ED) pattern obtained from (a) and (c) respectively. The ED patterns of (b) and (d) are indexed as metallic Fe and the ordered phase, respectively.